

# Atomic charges from IR intensity parameters: theory, implementation and application

Alberto Milani · Matteo Tommasini ·  
Chiara Castiglioni

Received: 26 May 2011 / Accepted: 28 August 2011 / Published online: 21 February 2012  
© Springer-Verlag 2012

**Abstract** A computational method to extract atomic charges (IR charges) from DFT/ab initio-computed atomic polar tensors is presented and compared with commonly available population schemes. The procedure adopted and its implementation in a (freely available) code are also reported and commented. Thanks to the procedure developed, infrared charges can be now readily gathered also by non-experts, provided that Cartesian dipole derivatives from a quantum chemical calculation of the IR spectrum are available. The method has been applied for the calculation of IR charges of about 50 molecules: It performs well in describing peculiar intramolecular interactions, providing a picture of the molecular charge distribution coherent with the chemical intuition. A nice agreement is also found with charges obtained from Hirshfeld algorithm and from the fitting of the electrostatic potential (CHELPG and MK schemes). On this basis, we propose IR charges as a reliable, physically sound and easily accessible alternative to other charge parameters currently adopted.

**Keywords** Atomic charges · Atomic polar tensor · DFT calculations · Infrared spectroscopy

## 1 Introduction

Atomic charge is probably one of the most elusive and arbitrarily defined molecular parameter. Its importance and usefulness is related to the fact that the structure, the

physical properties and the dynamics of molecular systems are deeply influenced by their charge distribution and by its modulation due to the supra-molecular environment or conformational changes. Moreover, a compact description of the charge distribution in terms of simple but effective parameters as point charges on nuclei may strongly improve our capability to recognize structure/properties correlations or to predict intermolecular interactions. In this respect, a significant example is that of amino acids and proteins, where the availability of accurate, geometry-dependent charges is mandatory for a reliable description of folding and of several intramolecular and intermolecular parameters affecting the dynamics of these complex systems [1–4].

This need is however quite general and concerns any molecular system and material, ranging from polymers to small molecules. Atomic charges are indeed used as essential parameters for the development of accurate force fields to be used in molecular dynamics simulations [5] (as, for instance, in the case of proteins, polymers or very large molecular assemblies), but they are also helpful for the rationalization of the structural characteristics and peculiar chemical/physical properties of small molecules *in vacuo*, for which they are usually derived from high-level first-principles simulations.

Since the birth of quantum chemistry, different schemes were proposed (e.g., Mulliken population analysis [6] and Lowdin population analysis [7, 8]) while others were developed or are currently developed based on the partitioning of the wave function or of the electronic density (natural population analysis [9, 10], atom-in-molecules (AIM) theory [11], Hirshfeld partitioning [12], Voronoi deformation density charges [13], etc.) or are based on the fitting of the molecular electrostatic potentials (ESP charges: MK [14, 15], Chelp [16], Chelpg [17], etc.). Many

A. Milani (✉) · M. Tommasini · C. Castiglioni  
Dipartimento di Chimica, Materiali e Ing. Chimica “G. Natta”,  
Politecnico di Milano, P.zza Leonardo da Vinci 32,  
20133 Milano, Italy  
e-mail: alberto.milani@polimi.it

papers compared the results obtained adopting different schemes, underlining the strength and the weakness of each of them [12, 18–23]. The charges obtained according to the methods mentioned above share an intrinsic and unavoidable weakness, since they cannot be directly related to any experimentally measurable property.

In the past, some models were developed for a parametrization of experimental infrared absorption intensities in terms of the equilibrium charges (or bond dipoles) and of their fluctuation during vibrational motions [24–34]. These “spectroscopy-oriented” models (electro-optical parameters (EOP) [26–28], equilibrium–charges–charge fluxes (ECCF) model [29–32], atomic polar tensors [33, 34]) were initially used mainly as tools for the rationalization of the observed infrared intensity patterns [24, 25] rather than to be applied for an effective description of the charge distribution in molecules. Only later, their importance in a broader context was recognized, and many applications were presented [25, 32, 35] especially for the ECCF model. In a parallel way and with a similar philosophy, some models aimed at extracting charge parameters were developed based on quantum chemically computed quantities related to spectroscopic observables. In particular, the modified version of the charge–charge flux–overlap (CCFO) model [31] (CCFOM model [36, 37]) was proposed as the theoretical counterpart of the ECCF model. The two models exploit the relationship existing between the derivatives of the molecular dipole moment with respect to Cartesian atomic displacement coordinates (namely atomic polar tensors, APTs) and ECCF parameters and introduce a definition of a suitable “correction” to Mulliken (net) charges, related to the so-called overlap contribution. More recently, new models as the charge–charge flux–dipole flux (CCFDF) model [38] have been proposed and applied to the interpretation and parametrization of IR intensity [39–41], demonstrating the evergreen interest on this topic of theoretical vibrational spectroscopy.

A step further in the application of charge parameters related to spectroscopy was made by Cioslowski, who introduced a straightforward definition of partial atomic charges based on APT invariants [42]. These charges, named generalized atomic polar tensor (GAPT) charges, can be readily calculated by standard quantum chemical codes; they satisfy both the symmetry requirement and the electroneutrality of the molecule, and they are directly related to experimentally measurable quantities (i.e., IR intensities). These features contributed to the success of GAPT charges as a model alternative to the most used and popular schemes.

In recent papers [43–45], we applied the ECCF model to calculate atomic charges from APTs obtained by density

functional theory (DFT) calculations. This can be done straightforwardly in the case of planar (or linear) molecules where atomic charges can be simply obtained for each atom ( $\beta$ ) by considering the out-of-plane  $yy$  diagonal element of the corresponding atomic polar tensor  $\mathbf{P}_\beta$ , namely  $q^\circ_\beta = P^\circ_{\beta yy}$ .

Notice that in the case of planar (or linear) molecules, Dinur [46] demonstrated that the above definition of atomic charge is unique from a theoretical perspective, a feature that confers to it a peculiar physical meaning. Unfortunately, the definition of the IR charge is exact [46] *only* in the case of planar (and linear) molecules, and it cannot be straightforwardly extended to the case of non-planar molecules. Moreover, for non-planar molecules, we cannot identify any given element of  $\mathbf{P}_\beta$  with  $q^\circ_\beta$ , and only approximated estimates of atomic charges can be obtained, according to ad hoc methods.

In [43], we proposed a method to obtain approximated IR charges of non-planar molecules, directly from a suitable element of APT, but our analysis was restricted to the case of (apex) H atoms, while a generalization of the method to different atoms and in particular to “internal” atoms has never been presented.

This is certainly one of the reasons of the little use of IR charges, which indeed have been applied in a very limited number of cases and only by a restricted number of experts in the field. Indeed, the lack of a general, standard procedure to get IR charges hinders their use as an investigatory tool, contrary to other popular schemes, which can be routinely used to obtain a description of the molecular charge distribution without the need to be an expert.

The development of a general procedure for the calculation of IR charges and its implementation in a computer code is the subject of this paper. We will discuss a method capable of providing approximated but reliable IR charges for all the atoms belonging to polyatomic, non-planar molecules.

In Sect. 2, the theory will be presented and described in detail. In Sect. 3, we will describe assumptions and choices adopted for the implementation of the model in the “Charges from IR Intensities” (CHIRI) program (freely available upon request to the authors).

Finally, in Sect. 4, charges calculated by means of the CHIRI program will be compared with those from some other methods by considering a wide set of molecules for which reliable IR intensity data are available (compared and discussed in [43]). The values of IR charges so calculated appear to be chemically sound, and they can be considered at least as reliable as other widely used approaches (e.g., Hirshfeld and CHELPG models).

## 2 Model and theory

Starting from the definition of the IR intensity  $I_i$  as a function of the dipole moment derivative  $\partial \vec{M} / \partial Q_i$  with respect to the normal mode coordinate  $Q_i$ , we can straightforwardly write its expression in terms of APTs, the tensors that collect the derivatives of the molecular dipole moment with respect to Cartesian atoms displacements  $\xi_k$ :

$$I_i = C |(\partial \vec{M} / \partial Q_i)^0|^2 = C |\sum_k (\partial \vec{M} / \partial \xi_k)^0 L_{ki}|^2 \quad (1)$$

where the “0” apex indicates values calculated at the equilibrium geometry,  $L_i$  is the eigenvector describing the relationship between Cartesian coordinates  $\xi_k$  and normal mode coordinate  $Q_i$ , and  $C$  is a constant depending on the adopted units.

Equation 1 shows that the first step required for any theoretical prediction of infrared intensities is the calculation of the set of parameters  $(\partial \vec{M} / \partial \xi_k)^0$ , which can be collected into  $N$  ( $N$  number of atoms in the given molecule)

$3 \times 3$  matrices, thus defining the APT,  $(P^\beta)_{ij} \equiv \left( \frac{\partial M_i}{\partial \xi_j^\beta} \right)^0$ .

On the one hand, APT values can be directly derived from the experimental IR intensity  $I_i$  by inversion of Eq. 1, provided that a reliable force field (and hence  $L_{ki}$  values) is available. Working on the expressions of the APT components as function of ECCF (or EOP), it is possible to extract local charge parameters and in particular to obtain the set of the atomic charges.<sup>1</sup> This task was accomplished in the past for a selected number of molecules and atoms [25, 32, 35], and it allowed a good description of several intra- and intermolecular chemical/physical properties [25, 32, 35, 47–53]. Anyway, severe limitations (such as the intrinsic difficulties related to absolute intensity determination, the presence of several overlapping bands, and the need of a good force field for the calculation of vibrational eigenvectors) hinder the direct determination of APT (or  $(\partial \vec{M} / \partial R_k)^0$ ) and thus of ECCF from experimental IR intensities.

On the other hand, APTs are always available when first-principles calculations of IR spectra are carried out: If a good agreement is found with the experimental IR intensity pattern, it is reasonable to consider the computed APTs as accurate counterparts of the experimental ones.

In a previous paper [43], we showed that DFT calculations (with a suitable choice of the exchange–correlation functional and basis set) can nicely reproduce the

experimental CH stretching IR intensities of about 50 molecules. Hydrogen atomic charges obtained from the DFT-computed APTs showed the capability to account for well-known chemical/physical effects. Moreover, their values are similar to those of other popular charges, such as charges derived from the fitting of the molecular electrostatic potential (ESP charges).

Once it is verified that the adopted level of theory provides a satisfactory prediction of IR intensities, we can focus on the computed APTs. The general  $uv$  component of the APT associated with the  $\beta$  atom can be written as:

$$P_{uv}^\beta = \left( \frac{\partial M_u}{\partial v_\beta} \right)^0 \quad (2)$$

The two indexes  $u$  and  $v$  respectively represent the  $x$ ,  $y$  or  $z$  component of the dipole moment and the  $x$ ,  $y$  or  $z$  Cartesian displacement of the  $\beta$  atom upon which the derivative of the dipole is carried out.

The theory of IR charges is founded on a basic hypothesis also adopted by other models (e.g., ESP charges), i.e. atomic charges  $q_\alpha$  are assumed to be spherically symmetric and are thus related to the molecular dipole moment  $\mathbf{M}$  according to:

$$\mathbf{M} = \sum_\alpha q_\alpha \mathbf{r}_\alpha^0 \quad (3)$$

where  $\mathbf{r}_\alpha$  is the position vector of the  $\alpha$  atom. By substituting Eq. 3 into 2, one obtains:

$$P_{uv}^\beta = q_\beta^0 \delta_{uv} + \sum_\alpha \left( \frac{\partial q_\alpha}{\partial v_\beta} \right)^0 u_\alpha^0 \quad (4)$$

where  $u_\alpha^0$  is the  $u$ th component of the equilibrium position vector  $\mathbf{r}_\alpha^0$ . This equation is general [under the assumption of Eq. 3] and describes any  $uv$  component of the APT.

It is possible to write Eq. 4 introducing charge fluxes parameters with respect to internal coordinates  $(R_i^\beta)$ . Accordingly, the three diagonal components of the APT of atom  $\beta$  become:

$$\begin{aligned} P_{xx}^\beta &= q_\beta^0 + \sum_\alpha \left( \frac{\partial q_\alpha}{\partial x_\beta} \right)^0 x_\alpha^0 = q_\beta^0 + \sum_\alpha \sum_t \left( \frac{\partial q_\alpha}{\partial R_t^\beta} \right)^0 \left( \frac{\partial R_t^\beta}{\partial x_\beta} \right)^0 x_\alpha^0 \\ P_{yy}^\beta &= q_\beta^0 + \sum_\alpha \left( \frac{\partial q_\alpha}{\partial y_\beta} \right)^0 y_\alpha^0 = q_\beta^0 + \sum_\alpha \sum_t \left( \frac{\partial q_\alpha}{\partial R_t^\beta} \right)^0 \left( \frac{\partial R_t^\beta}{\partial y_\beta} \right)^0 y_\alpha^0 \\ P_{zz}^\beta &= q_\beta^0 + \sum_\alpha \left( \frac{\partial q_\alpha}{\partial z_\beta} \right)^0 z_\alpha^0 = q_\beta^0 + \sum_\alpha \sum_t \left( \frac{\partial q_\alpha}{\partial R_t^\beta} \right)^0 \left( \frac{\partial R_t^\beta}{\partial z_\beta} \right)^0 z_\alpha^0 \end{aligned} \quad (5)$$

where the terms  $\left( \frac{\partial R_t^\beta}{\partial x_\beta} \right)^0$  are the suitable elements of the  $\mathbf{B}$  matrix, which defines the relationship between the internal and the Cartesian coordinates systems ( $\mathbf{R} = \mathbf{B}\xi$ ), according to Wilson [54].

<sup>1</sup> Notice that an equivalent (most commonly followed) method for the determination of ECCF parameters from experimental intensities is the parametrization of the set  $(\partial \vec{M} / \partial R_k)^0$ , namely dipole derivatives with respect to internal (valence) coordinates, which are related to infrared intensities by a suitable relationship, formally similar to Eq. 1.

Looking at Eq. 5, we can immediately realize that each diagonal APT component contains two terms: the atomic charge ( $q_\beta^0$ ) of the  $\beta$  atom and a sum of charge fluxes ( $\frac{\partial q_\alpha}{\partial R_i^\beta}$ ) over all the atoms of the molecule, induced by displacements of the whole subset of internal coordinates  $R_i^\beta$ , involving the  $\beta$  atom.<sup>2</sup>

Our main goal relies on finding a suitable way to extract from Eq. 5 the atomic charge  $q_\beta^0$ . The structure of Eq. 5 suggests that a rotation of the APT in a suitable Cartesian reference system could provide a very simple expression for some APT components in terms of a few parameters. This happens for *planar* molecules, where a suitable Cartesian reference system can be defined exploiting the molecular symmetry. If the  $y$  axis is chosen orthogonal to the molecular plane, the relationship  $y_\alpha^0 \equiv 0$ ,  $\forall \alpha$  atom is verified and the  $yy$  component of Eq. 5 assumes the following appealing form:

$$P_{yy}^\beta = q_\beta^0 = q_\beta^{IR} \quad (6)$$

This states the identity between the charge of the  $\beta$  atom and the  $yy$  element of APT. The charges so obtained can be defined “infrared (IR) charges”  $q_\beta^{IR}$ , since Eqs. 6 and 1 immediately show the existing correlation with IR absorption intensities.

In addition, Eq. 6 offers the way to obtain theoretical atomic charges directly from computed APTs, provided that the molecule is planar (or linear) and Eq. 3 holds. On these grounds, “IR charges” can be considered “exact,” as proved by Dinur [46].

Notice that relaxing the hypothesis stated by Eq. 3 would imply the explicit introduction of atomic dipoles, reflecting the fact that atoms in molecules do not have a spherical charge distribution. This hypothesis has been introduced by the CCFDF model [38], where atomic dipoles and their fluxes are determined according to the AIM theory [11]. Unfortunately, models including multipolar terms give rise to equations containing a large number of unknowns, a fact that does not allow to determine unique values of the whole set of point atomic charges *and* atomic dipoles, even in the case of small planar molecules [46].

A direct consequence of a definition of charges based on Eq. 3 is that they allow to exactly reproduce the molecular dipole moment of the molecule, a feature which is mandatory (but not respected by some other popular charge definitions, e.g., GAPT charges) for a reliable description

of molecular charge distribution strictly based on partial atomic charges.

The main weakness of the above definition of IR charges relies in the fact that it cannot be straightforwardly transferred to non-planar molecules, because for these molecules, there is not a plane which makes Eq. 6 true. In other words, independently on the Cartesian reference system adopted, charge flux terms appearing in Eq. 5 can give non-negligible contributions, thus preventing the identification of the atomic charge with a particular APT component.

In order to extend the use of Eq. 6 to *non-planar* molecules, the *local plane approximation* has been introduced in a previous paper [43]. According to this model, we can select a plane defined by the position of the  $\beta$  atom and two other neighboring atoms: By a suitable rotation of the Cartesian reference system, we can put the  $y$  axis perpendicular to this plane. Let us now consider the  $P_{yy}^\beta$  component of the tensor  $\mathbf{P}^\beta$  expressed in this reference system: We can use again Eq. 6 to define the (approximate) atomic charge of the  $\beta$  atom, if the charge fluxes appearing in its analytic expression (see Eq. 5) are small enough to be neglected. Under this regard, it is important to notice that only charge flux terms occurring on atoms lying out of the local plane ( $y_\alpha^0 \neq 0$ ) can enter in the expression of  $P_{yy}^\beta$ , so fluxes on the  $\beta$  atoms and on the neighboring atoms selected for the definition of the local plane do not affect the value  $P_{yy}^\beta$ . Moreover, fluxes related to internal coordinates which do not involve displacements of the  $\beta$  atom out of the local plane cannot appear in the expression of  $P_{yy}^\beta$ . Indeed, fluxes induced by stretchings, as well as bendings occurring in the local plane, vanish by virtue of the relationship:  $\left(\frac{\partial R_i^\beta}{\partial y_\beta}\right)^0 = 0$ .

The main problem is now to find the “best” local plane that makes Eq. 6 as good as possible, minimizing the charge flux contributions.

Generally speaking, different atoms require to select different planes (and to carry out the rotation of the corresponding APT), with the only exception of planar molecules where for each atom the best local plane coincides with the univocally defined symmetry plane of the molecule.

In several cases, it is rather straightforward to choose a local plane: For instance, in the case of planar chemical fragments (e.g., in the presence of  $sp^2/sp$  carbon atoms occurring in non-planar molecules), the local plane should be immediately identified with the plane of the fragment. It can be shown that in this case, charge fluxes are simply related to out-of-plane bendings or torsional valence coordinates and can be reasonably neglected due to the local symmetry (this happens, for instance, for C–OH and COOH groups [44]).

<sup>2</sup> This partitioning is exactly the same followed by CCFOM model [36, 37] where corrected Mulliken atomic charges and the associated charge fluxes are defined considering the analytic expressions of APT components.



A similar argument holds for linear fragments occurring in a non-planar molecule, for which the local plane can be chosen in the infinite set of planes, which contains the linear sequence of atoms: Also in this case, based on local symmetry, fluxes associated with linear bendings can be considered negligible.

According to the above observations, we can conclude that Eq. 6 would be applied with confidence for the determination of the equilibrium charges of apex atoms attached to  $sp^2$  (and  $sp$ ) carbons, also when they belong to non-planar molecules.

However, especially for “internal” atoms connected to more than three atoms (as for instance  $sp^3$  carbons), there is not a simple way to guess the importance of the different charge flux parameters and, therefore, a general rule that guarantees to obtain a good (approximated) IR charge is lacking.

In order to overcome this problem, we have developed a method, based on the introduction of suitable correction parameters; the method has been implemented in a computer code (CHIRI program) and will be discussed in detail in the next Section.

### 3 Implementation

#### 3.1 Determination of the local plane

As indicated above, the choice of the best local planes cannot be done on general grounds, while different strategies can be suggested. In a previous paper [43] focusing on hydrogen charges, all the local planes have been identified by choosing as the second atom (A) the one covalently bonded to H and by selecting a second neighboring atom (atom B, bonded to A and, if possible, different from an hydrogen) as the third atom. This choice was based on previous experience showing that the large non-principal charge fluxes<sup>3</sup> often involve atoms with many electrons.

As an alternative strategy for the definition of the local plane, another “special” plane could be selected, in such a way that all the atoms distances  $y_\alpha^0$  are minimized. This property is obviously satisfied for a planar molecule when considering the molecular plane, since in this case, by definition,  $y_\alpha^0 \equiv 0, \forall \alpha$ . Even if this choice is suitable for implementation in a computer program, there are some

drawbacks that make it not acceptable: In particular, it does not guarantee the effective cancellation of the major charge flux terms. Indeed, principal stretching charge fluxes (whose values are often one order of magnitude larger than the other fluxes) can enter in this case in the expression of  $P_{yy}^\beta$ , possibly introducing a relevant error even if they are weighted by a small  $y_\alpha^0$ .

Furthermore, atoms far from the  $\beta$  atom are expected to contribute with negligible charge fluxes to  $P_{yy}^\beta$ , thus suggesting that the minimization of the  $y_\alpha^0$  distances should be restricted only to atoms “close” to the  $\beta$  atom; this fact again introduces some arbitrariness in the choice of the plane because it requires the definition of a threshold  $\alpha$ – $\beta$  distance.

A further possibility for the determination of the local plane is based on a criterion of maximum similarity with respect to the case of a planar molecule: For such a molecule indeed, it results  $P_{xy} = P_{yx} = P_{yz} = P_{zy} = 0$  (provided that the y axis is orthogonal to the molecular plane). In principle, in non-planar molecules, the APT components referred to the best local plane should be as similar as possible to the case of a planar molecule. To this aim, one can define the parameter  $\sigma$  as

$$\sigma = \frac{1}{4} \sqrt{(P_{xy}^\beta)^2 + (P_{yx}^\beta)^2 + (P_{yz}^\beta)^2 + (P_{zy}^\beta)^2}$$

where the terms under the square root are the APT components associated with the  $\beta$  atom rotated in the system of reference of the local plane under investigation (which is orthogonal to y). By minimization of  $\sigma$ , one could find the best local plane giving the most accurate value of the IR charge. This procedure would be straightforward to implement and unsupervised; however, there are serious drawbacks for its application. In the presence of symmetry or local symmetry, the local plane showing the lowest (or even zero!) value of  $\sigma$  is not necessarily the one which minimizes the contribution of charge fluxes to the diagonal  $P_{yy}^\beta$  component. Indeed, the shape of the polar tensor is determined by the symmetry of the site. Taking for instance the case of the  $CH_2F_2$  molecule and considering  $\beta = H$ , one finds that the H–C–H local plane is the one showing the least value of  $\sigma$  (in particular,  $\sigma = 0$ ). This happens because this plane is a mirror symmetry plane of the molecule and  $P_{yx} = -P_{xy} = 0, P_{xy} = -P_{yx} = 0, P_{yz} = -P_{zy} = 0, P_{zy} = -P_{yz} = 0$ , namely  $\sigma = 0$ . In spite of this, the above choice does not prevent that large bending charge fluxes toward the two out-of-plane F atoms affect the  $P_{yy}^H$  element.

For the above reasons, we decided to adopt (and to implement in the CHIRI program) a pragmatic approach: Accordingly, for each  $\beta$  atom under investigation, a local plane defined by the three atoms  $\beta$ , A and B must be selected by the user. This supervised procedure obviously requires a minimum background knowledge by the user;

<sup>3</sup> Charge fluxes induced on the atom  $\beta$  by the stretching of a covalent bond  $X\beta$  are usually referred to as principal charge fluxes. Principal (stretching) charge fluxes are usually larger (often by one order of magnitude) than non-principal fluxes (e.g. bending fluxes), independently from the nature of the element  $\beta$ . Notice, moreover, that according to its definition, any local plane for an H atom contains the H–X bond and the principal charge flux can contribute only to the  $P_{zz}^H$  element (with the z axis lying along the H–X bond).

however, it can safely avoid many wrong choices which could be hidden in the automatic procedures previously described.

The local plane should be chosen according to the following rules:

1. the plane must contain the  $\beta$  atom, and one of the atoms covalently bonded to it (one nearest neighbor, A);
2. the third atom (B) is another atom directly bonded to  $\beta$ ; otherwise, for monovalent  $\beta$  atoms, it has to lie two bonds away from  $\beta$  (first or second neighbor, B);
3. whenever it is possible, the B atom must be different from hydrogen.

According to the choice of the local plane, a Cartesian reference system is defined with the  $z$  axis along the  $\beta$ -A bond, the  $x$  axis orthogonal to  $z$  (and lying in the  $\beta$ -A-B local plane) and the  $y$  axis orthogonal to the plane.

Depending on the molecule considered, for any given atom, it may happen that different choices of the  $\beta$ -A-B sequence can be made: They can be equivalent or non-equivalent, according to the molecular symmetry. For instance, in the case of propane, methylene hydrogen atoms of two different HCC sequences define equivalent planes which will give identical values of  $P_{yy}^H$ ; thus, the definition of  $q_{\beta}^{IR}$  is unambiguous. Instead, in the case of butane methylene hydrogen atoms, the carbon atom of one adjacent methyl unit can be chosen as the B atom, as well as the carbon atom belonging to the other methylene group and the two choices of B define two different non-equivalent local planes. Even more complex situations can be found when considering “inner” atoms, as for instance carbon atoms in  $sp^3$  hybridization for which there is a manifold of possible choices of local planes.

However, independently on the choice made, the procedure illustrated above guarantees that:

- the local plane always contain the bond  $\beta$ -A, thus avoiding that the principal charge flux related to the stretching of the  $\beta$ -A bond contributes to  $P_{yy}^{\beta}$ ;
- charge flux contributions relative to A and B atoms (neighbors of  $\beta$ ) do not appear in  $P_{yy}^{\beta}$  because they are canceled thanks to the identities  $y_A^0 = y_B^0 = 0$ .

Once a suitable local plane is selected for each atom in the molecule, a preliminary set of charges is determined by the application of Eq. 6. The set of  $P_{yy}^{\beta}$  (each of them referred to the local plane selected for the given  $\beta$  atom) represents the first guess, *uncorrected* atomic charge on  $\beta$ ,  $q_{\beta}^{IR, uncorr}$  (Eq. 6).

### 3.2 Correction and determination of the final set of IR charges

The charges so obtained are approximated IR charges, and we are not guaranteed that the electroneutrality of the molecule and the molecular dipole moment are correctly reproduced by the set of  $q_{\beta}^{IR, uncorr}$ . This suggests to introduce a correction procedure, which can be applied to those charges which are expected to be more seriously affected by charge flux contributions (i.e., inner atoms with non-planar coordination or apex atoms different from hydrogen, bonded to  $sp^3$  carbons).

The conditions to be fulfilled are namely:

$$\sum_{\alpha} q_{\alpha}^{IR} = 0 \quad (\text{charge neutrality}) \quad (8)$$

$$\sum_{\alpha} q_{\alpha}^{IR} \mathbf{r}_{\alpha} = \mathbf{M}_{calc} \quad (\text{dipole moment}) \quad (9)$$

where  $\mathbf{M}_{calc}$  is the first-principles computed dipole moment.

In the most general case, Eqs. 8 and 9 give four equations that can be used to determine four correction parameters. This allows us to define the set of atoms to be corrected, which in turns are grouped into four subsets, whose members will be corrected by the same amount  $a_i$  to give the final IR charges:

$$q_{\beta,i}^{IR} = q_{\beta,i}^{IR, uncorr} + a_i = P_{yy}^{\beta,i} + a_i \quad (10)$$

In Eq. 10,  $i$  is the “subset number” ( $i = 1, 2, 3$  or  $4$ ) which identifies the four correction parameters  $a_1, a_2, a_3$  and  $a_4$  to be determined by assuming Eq. 10 and solving the system of equations given by Eqs. 8 and 9.

The following advices should guide the definition of these subsets, namely:

1. Atoms equivalent by symmetry must be collected in the same subset. Notice that in these cases, the first guess uncorrected IR charges of equivalent atoms should be identical, since local planes of equivalent atoms have to be selected following a symmetry criterion.
2. Atoms of different chemical nature should be assigned to different subsets: Indeed, there is no reason justifying the introduction of an identical correction in these cases.
3. Non-equivalent atoms of the same chemical nature could be grouped in the same subset, especially if the chemical environment is similar.

Notice that the possible number of correction parameters (and therefore the number of subsets) decreases in the case of symmetric molecules, where some dipole components vanish for symmetry reasons (for instance, in the presence

of inversion center, the whole equilibrium molecular dipole is zero).

## 4 Application

### 4.1 Computational details

The accuracy of IR charges is related to the choice of a good theoretical method for the calculation of IR intensities: In [43], the performances of some DFT functionals and basis sets were discussed, and it was found that the combination PBE0 [55]/aug-cc-pVTZ gave the best prediction of CH stretching intensities. As a valuable alternative, PBE0/6-311++G\*\* resulted to be the best compromise when an accurate prediction of IR intensity is required at a slightly lower computational cost. However, our investigation was not exhaustive and should be reconsidered as far as new DFT functionals appear, pushed by the call for increased accuracy.

Based on the previous good results, we will consider in this work just IR charges derived from APT computed at PBE0/aug-cc-pVTZ level of theory.

All the calculations here presented have been carried out by using Gaussian 03 and Gaussian 09 codes [56, 57]. Mulliken [6], MK [14, 15], CHELPG [17], GAPT [42], Hirshfeld [12] and NPA [9, 10] charges have been calculated as implemented in Gaussian. APT has been extracted from the output of the IR spectra calculation and has been used as input for the CHIRI program for the calculation of IR charges. The CHIRI Fortran code has been entirely written by the authors.

It should be noted that IR charges (but also GAPT charges) show a non-negligible weakness due to the high computational demand required for their calculation: Being derived from the APT components, they can be obtained *only if* the calculation of the IR spectrum is carried out, while ESP charges, as well as charges derived by other population schemes, simply require a preliminary geometry optimization. This fact could seriously hinder the calculation of IR charges in the case of very large systems.

### 4.2 Results and discussion

DFT-derived IR charges of hydrogen atoms are in very good agreement with previously derived experimental IR charges and provide a good interpretation of effects such as charge backdonation from oxygen or nitrogen lone pairs, hyperconjugation with  $\pi$  electrons systems and inductive effects by neighboring electronegative atoms. On the basis of IR charges on hydrogen, it is possible to guess its ability to form hydrogen bonds. Furthermore, it is known since long time that IR charges show a good agreement with ESP charges [37, 43].

In Table 1, IR charges are compared to orbital-based charges (Mulliken and NPA), to ESP charges (calculated according to the MK and CHELPG schemes), to charges obtained from the Hirshfeld partitioning and to GAPT charges. In Fig. 1, we report correlation plots of IR charges with respect to the other kinds of charge here considered.

By examining the plots of Fig. 1, it is possible to get an overall idea of the similarity of the description of the charge distributions resulting from the different methods. In addition, in Table 2, the root-mean-squared (RMS) deviation and the mean absolute deviation (MAD) of the IR charges versus the other kinds of charge are reported.

The best global agreement with IR charges is obtained by Hirshfeld and CHELPG charges: This is a valuable result since these two schemes have been successfully applied for a large variety of molecular systems, showing a good ability to describe trends following the chemical intuition [12, 19, 21]. This holds in particular for Hirshfeld charges, and it is described in detail in a couple of papers [13, 21].

For the other methods, IR charges show larger discrepancies especially when compared with GAPT charges. At first sight, this is quite surprising since both GAPT and IR charges are deduced from computed APT.

A thorough comparison between GAPT and IR charges, focusing both on the theoretical definitions and on numerical values, has been recently presented and applied to the case of halogen-substituted ethylenes [45]: It has been shown that in the definition of GAPT charges, a consistent contribution due to charge fluxes is present which largely affects their numerical values, making them hardly transferable between chemically similar molecules. In addition, GAPT charges do not reproduce the molecular dipole moment of the molecule, a fact that further weakens their applicability.

It should be noted that a good agreement between GAPT and IR charges is found in the case of very undeformable charge distributions, that is, when charge fluxes are all very small; in these cases, the definition of atomic charge according to the two methods coincides. Undeformable charges are found in some peculiar cases [32] as for instance hydrogen atoms able to form hydrogen bonds, such as HCN and  $C_2H_2$ : Indeed, in these cases, the IR charges (Table 1) of the H atoms are respectively +0.258 and +0.218 e, in very good agreement with GAPT charges (+0.257 and +0.218 e respectively). The same behavior is also found with other molecules forming H bond, such as  $CH_3-C\equiv C-H$ , showing very similar IR and GAPT charges on the H atom belonging to the C(sp)H bond. On the other side, for conjugated sp systems (e.g.,  $C_nH_2$ ), GAPT and IR charges differ, because of the contribution of non-negligible charge fluxes taking place along the conjugated carbon chain. Already for  $C_4H_2$ , the IR and GAPT charges start to show some discrepancy (0.212 vs. 0.234 e). On the other

**Table 1** Comparison of atomic charges obtained by using the method presented in Sect. 2 (IR charges) and atomic charges obtained with other popular schemes. All calculations have been done at PBE0/aug-cc-pVTZ level of theory, and all units are electron charge

q (e) →		IR	CHELPG	MK	NPA	Hirshfeld	GAPT	Mulliken	Index
HCN	C	0.055	0.169	0.123	0.074	0.059	−0.053	−0.353	1
	H	0.258	0.199	0.223	0.225	0.13	0.257	0.638	2
	N	−0.313	−0.368	−0.346	−0.299	−0.189	−0.204	−0.285	3
C <sub>2</sub> H <sub>2</sub>	C	−0.218	−0.232	−0.28	−0.233	−0.096	−0.215	−0.573	4
	H	0.218	0.232	0.28	0.233	0.096	0.215	0.573	5
C <sub>4</sub> H <sub>2</sub>	C(CH)	−0.184	−0.336	−0.388	−0.142	−0.066	−0.288	−1.096	6
	C	−0.028	0.078	0.084	−0.096	−0.034	0.054	0.771	7
	H	0.212	0.258	0.304	0.238	0.1	0.234	0.325	8
CH <sub>3</sub> −CN	C(CH <sub>3</sub> )	−0.108	−0.291	−0.509	−0.718	−0.054	0.062	−0.503	9
	C(CN)	0.102	0.409	0.449	0.282	0.076	0.131	0.055	10
	N	−0.333	−0.498	−0.495	−0.325	−0.236	−0.328	−0.357	11
CH <sub>3</sub> CCH	H	0.113	0.127	0.185	0.254	0.071	0.045	0.268	12
	C	−0.132	0.056	0.227	−0.004	−0.051	0.013	0.684	13
	C(CH)	−0.26	−0.439	−0.601	−0.26	−0.133	−0.359	−1.281	14
CH <sub>3</sub> −C <sub>2</sub> −CN <sup>a</sup>	C(CH <sub>3</sub> )	−0.13	−0.067	−0.421	−0.683	−0.071	0.088	−0.669	15
	H <sub>(1)</sub>	0.221	0.263	0.34	0.234	0.085	0.216	0.488	16
	H <sub>(2)</sub>	0.1	0.062	0.151	0.238	0.057	0.014	0.259	17
	C <sub>(1)</sub>	−0.032	−0.282	−0.449	−0.174	−0.047	−0.275	1.372	18
	C <sub>(2)</sub>	−0.032	0.078	0.291	0.158	0.017	0.194	−1.241	19
	C <sub>(3)</sub>	0.202	0.53	0.578	0.212	0.082	0.366	0.417	20
	C <sub>(4)</sub>	−0.148	−0.086	−0.481	−0.696	−0.06	0.001	−0.767	21
CH <sub>3</sub> −C <sub>2</sub> −CH <sub>3</sub>	H	0.111	0.083	0.18	0.252	0.069	0.028	0.258	22
	N	−0.324	−0.487	−0.477	−0.257	−0.198	−0.37	−0.554	23
	C	−0.187	−0.158	−0.071	−0.026	−0.078	−0.118	0.053	24
	C(CH <sub>3</sub> )	−0.099	0.071	−0.342	−0.669	−0.077	0.125	−0.764	25
	H	0.096	0.029	0.138	0.232	0.052	−0.003	0.237	26
CH <sub>2</sub> =C=CH <sub>2</sub>	C	−0.058	0.216	0.264	0.096	−0.005	0.158	0.594	27
	C(CH <sub>2</sub> )	−0.305	−0.463	−0.582	−0.498	−0.109	−0.204	−0.909	28
	H	0.167	0.177	0.225	0.225	0.055	0.062	0.306	29
C <sub>2</sub> H <sub>4</sub>	C	−0.298	−0.252	−0.327	−0.382	−0.086	−0.074	−0.711	30
	H	0.149	0.126	0.164	0.191	0.043	0.037	0.355	31
CH <sub>2</sub> CF <sub>2</sub>	C(CH <sub>2</sub> )	−0.383	−0.655	−0.742	−0.601	−0.14	−0.353	−0.913	32
	C(CF <sub>2</sub> )	0.151	0.535	0.532	0.754	0.178	1.175	0.646	33
	H	0.179	0.232	0.267	0.229	0.059	0.096	0.333	34
C <sub>2</sub> H <sub>2</sub> F <sub>2</sub> trans	F	−0.063	−0.172	−0.162	−0.306	−0.078	−0.507	−0.2	35
	C	−0.091	−0.014	−0.055	0.147	0.031	0.395	−0.207	36
	H	0.198	0.17	0.191	0.174	0.066	0.081	0.568	37
C <sub>2</sub> H <sub>2</sub> F <sub>2</sub> cis	F	−0.107	−0.156	−0.136	−0.321	−0.098	−0.476	−0.361	38
	C	−0.102	−0.012	−0.042	0.139	0.029	0.398	−0.216	39
	H	0.17	0.121	0.137	0.176	0.063	0.069	0.525	40
C <sub>2</sub> H <sub>2</sub> Cl <sub>2</sub> trans	F	−0.068	−0.109	−0.095	−0.315	−0.092	−0.467	−0.309	41
	C	−0.135	−0.069	−0.12	−0.24	0.001	0.232	−0.25	42
	H	0.167	0.158	0.187	0.222	0.067	0.061	0.44	43
C <sub>2</sub> H <sub>2</sub> Cl <sub>2</sub> cis	Cl	−0.032	−0.089	−0.067	0.018	−0.068	−0.293	−0.19	44
	C	−0.144	−0.073	−0.138	−0.252	−0.003	0.176	−0.247	45
	H	0.169	0.127	0.166	0.225	0.066	0.053	0.387	46
	Cl	−0.025	−0.054	−0.028	0.027	−0.063	−0.229	−0.139	47



**Table 1** continued

q (e) →		IR	CHELPG	MK	NPA	Hirshfeld	GAPT	Mulliken	Index
Butadiene <sup>b</sup>	C <sub>(1)</sub>	−0.291	−0.392	−0.44	−0.363	−0.088	−0.137	−0.935	48
	C <sub>(2)</sub>	−0.134	0.004	−0.057	−0.223	−0.043	0.039	−0.014	49
	H <sub>(3)</sub>	0.137	0.086	0.139	0.199	0.046	0.022	0.296	50
	H <sub>(4)</sub>	0.148	0.157	0.184	0.189	0.042	0.037	0.275	51
	H <sub>(5)</sub>	0.14	0.145	0.174	0.198	0.043	0.039	0.378	52
C <sub>6</sub> H <sub>6</sub>	C	−0.134	−0.078	−0.126	−0.21	−0.045	−0.035	−0.476	53
	H	0.134	0.078	0.126	0.21	0.045	0.035	0.476	54
CH <sub>2</sub> O	C	0.134	0.442	0.377	0.279	0.129	0.667	−0.293	55
	H	0.093	−0.011	0.011	0.103	0.048	−0.045	0.346	56
	O	−0.32	−0.42	−0.399	−0.485	−0.225	−0.578	−0.399	57
HFCO	C	0.351	0.616	0.574	0.713	0.234	1.151	0.146	58
	H	0.116	0.02	0.035	0.113	0.079	0.034	0.421	59
	F	−0.146	−0.216	−0.205	−0.329	−0.095	−0.569	−0.236	60
	O	−0.321	−0.42	−0.404	−0.497	−0.218	−0.616	−0.331	61
Propylene <sup>c</sup>	C <sub>(1)</sub>	−0.299	−0.412	−0.547	−0.391	−0.104	−0.151	−0.874	62
	C <sub>(2)</sub>	−0.243	−0.014	0.08	−0.182	−0.038	0.064	−0.296	63
	C <sub>(3)</sub>	−0.131	−0.041	−0.308	−0.656	−0.097	0.036	−0.558	64
	H <sub>(1)</sub>	0.151	0.075	0.081	0.191	0.039	0.012	0.407	65
	H <sub>(2)</sub>	0.142	0.168	0.217	0.186	0.039	0.031	0.318	66
	H <sub>(3)</sub>	0.148	0.137	0.18	0.195	0.038	0.032	0.313	67
	H <sub>(4)</sub>	0.083	0.023	0.089	0.214	0.039	−0.006	0.215	68
	H <sub>(5)</sub>	0.074	0.032	0.104	0.222	0.042	−0.008	0.237	69
Isobutene	C	−0.12	0.334	0.49	0.004	0.004	0.149	0.616	70
	C(CH <sub>2</sub> )	−0.334	−0.57	−0.677	−0.402	−0.116	−0.199	−1.009	71
	C(CH <sub>3</sub> )	−0.162	−0.304	−0.563	−0.636	−0.096	0.028	−0.798	72
	H(CH <sub>2</sub> )	0.15	0.176	0.212	0.19	0.034	0.028	0.307	73
	H(CH <sub>3</sub> <sup>opla</sup> )	0.083	0.082	0.148	0.214	0.039	−0.011	0.231	74
	H(CH <sub>3</sub> <sup>inpla</sup> )	0.073	0.081	0.148	0.216	0.04	−0.009	0.225	75
	C	−0.202	0.025	0.144	−0.022	−0.014	0.037	0.82	76
Tetramethyl-ethylene	C(CH <sub>3</sub> )	−0.113	−0.199	−0.422	−0.621	−0.099	0.036	−1.072	77
	H(CH <sub>3</sub> <sup>inpla</sup> )	0.068	0.061	0.111	0.21	0.035	−0.002	0.281	78
	H(CH <sub>3</sub> <sup>opla</sup> )	0.073	0.063	0.119	0.211	0.036	−0.026	0.191	79
	C	0.019	−0.114	−0.204	−0.106	−0.004	0.285	−0.366	80
Ethylene oxide	H	0.058	0.115	0.153	0.18	0.048	−0.008	0.315	81
	O	−0.272	−0.232	−0.205	−0.506	−0.184	−0.537	−0.527	82
CH <sub>4</sub>	C	−0.276	−0.396	−0.544	−0.846	−0.144	−0.02	−0.976	83
	H	0.069	0.099	0.136	0.212	0.036	0.005	0.244	84
CH <sub>3</sub> F	C	−0.003	0.142	−0.047	−0.115	0.013	0.547	−0.378	85
	H	0.072	0.034	0.084	0.162	0.045	−0.015	0.247	86
	F	−0.215	−0.244	−0.205	−0.37	−0.149	−0.502	−0.362	87
CH <sub>2</sub> F <sub>2</sub>	C	0.396	0.391	0.278	0.446	0.14	1.095	0.123	88
	H	0.03	0.031	0.063	0.126	0.054	−0.025	0.255	89
	F	−0.228	−0.227	−0.202	−0.349	−0.124	−0.523	−0.317	90
CHF <sub>3</sub>	C	0.653	0.553	0.536	0.882	0.247	1.591	0.567	91
	H	0.017	0.047	0.052	0.104	0.065	−0.015	0.274	92
	F	−0.223	−0.2	−0.196	−0.329	−0.104	−0.525	−0.28	93

**Table 1** continued

q (e) →		IR	CHELPG	MK	NPA	Hirshfeld	GAPT	Mulliken	Index
CH <sub>3</sub> Cl	C	−0.1	−0.191	−0.489	−0.557	−0.025	0.27	−0.541	94
	H	0.091	0.117	0.2	0.211	0.054	0.004	0.246	95
	Cl	−0.174	−0.16	−0.111	−0.076	−0.138	−0.282	−0.198	96
CH <sub>2</sub> Cl <sub>2</sub>	C	0.259	−0.144	−0.488	−0.389	0.063	0.606	−0.145	97
	H	0.029	0.153	0.259	0.215	0.066	−0.002	0.254	98
	Cl	−0.159	−0.081	−0.015	−0.021	−0.098	−0.301	−0.181	99
CHCl <sub>3</sub>	C	0.601	−0.179	−0.482	−0.295	0.136	0.955	0.185	100
	H	−0.061	0.198	0.299	0.214	0.072	−0.022	0.254	101
	Cl	−0.18	−0.006	0.061	0.027	−0.069	−0.311	−0.146	102
CH <sub>3</sub> Br	C	−0.112	// <sup>g</sup>	−0.69	−0.641	−0.03	0.198	−0.655	103
	H	0.09	//	0.254	0.216	0.063	0.005	0.237	104
	Br	−0.158	//	−0.073	−0.008	−0.158	−0.214	−0.056	105
CH <sub>3</sub> OH <sup>d</sup>	C	−0.052	0.242	0.097	−0.237	−0.02	0.463	−0.507	106
	H(G)	0.08	0.036	0.074	0.182	0.043	−0.007	0.28	107
	H(T)	0.062	−0.027	0.011	0.158	0.03	−0.052	0.241	108
	O	−0.488	−0.604	−0.577	−0.721	−0.239	−0.598	−0.4	109
	H(OH)	0.337	0.38	0.384	0.459	0.156	0.247	0.146	110
	C	−0.048	0.049	−0.08	−0.232	−0.017	0.487	−0.603	111
(CH <sub>3</sub> ) <sub>2</sub> O <sup>d</sup>	H(T)	0.055	0.03	0.064	0.16	0.03	−0.054	0.26	112
	H(G)	0.078	0.052	0.086	0.189	0.044	−0.009	0.283	113
	O	−0.281	−0.323	−0.268	−0.556	−0.172	−0.741	−0.4	114
	C	−0.083	−0.074	−0.324	−0.391	−0.056	0.339	−0.785	115
(CH <sub>3</sub> ) <sub>3</sub> N <sup>e</sup>	H(eq)	0.071	0.07	0.134	0.198	0.036	−0.018	0.256	116
	H(ax)	0.042	0.041	0.108	0.164	0.017	−0.084	0.242	117
	N	−0.304	−0.32	−0.158	−0.505	−0.098	−0.659	0.093	118
	C	−0.21	−0.02	−0.041	−0.6	−0.099	0.072	−0.666	119
Ethane	H	0.07	0.007	0.014	0.2	0.033	−0.024	0.222	120
	C(CH <sub>3</sub> )	−0.237	−0.231	−0.324	−0.596	−0.1	0.054	−0.748	121
Propane	C	−0.014	0.298	0.327	−0.403	−0.058	0.121	−0.197	122
	H(CH <sub>3</sub> <sup>impla</sup> )	0.073	0.04	0.065	0.206	0.033	−0.025	0.211	123
	H(CH <sub>3</sub> <sup>opla</sup> )	0.067	0.048	0.073	0.199	0.032	−0.022	0.23	124
	H(CH <sub>2</sub> )	0.037	−0.054	−0.05	0.193	0.032	−0.046	0.176	125
	C(CH <sub>3</sub> )	−0.157	−0.285	−0.38	−0.594	−0.1	0.06	−0.802	126
Butane	C(CH <sub>2</sub> )	−0.125	0.154	0.168	−0.396	−0.059	0.1	−0.219	127
	H(CH <sub>3</sub> <sup>impla</sup> )	0.073	0.069	0.096	0.206	0.033	−0.028	0.2	128
	H(CH <sub>3</sub> <sup>opla</sup> )	0.066	0.057	0.081	0.199	0.032	−0.022	0.221	129
	H(CH <sub>2</sub> )	0.038	−0.026	−0.022	0.193	0.031	−0.044	0.19	130
	C <sub>(1)</sub>	−0.195	−0.169	−0.248	−0.593	−0.1	0.058	−0.833	131
Pentane <sup>f</sup>	C <sub>(2)</sub>	−0.047	0.151	0.16	−0.393	−0.059	0.107	−0.3	132
	C <sub>(3)</sub>	−0.146	−0.047	−0.03	−0.393	−0.059	0.076	−0.134	133
	H <sub>(1)</sub>	0.066	0.04	0.064	0.206	0.033	−0.031	0.205	134
	H <sub>(2)</sub>	0.073	0.03	0.05	0.199	0.032	−0.021	0.218	135
	H <sub>(3)</sub>	0.038	−0.033	−0.033	0.193	0.031	−0.044	0.176	136
	H <sub>(4)</sub>	0.034	0.008	0.005	0.193	0.03	−0.042	0.206	137

**Table 1** continued

q (e) →		IR	CHELPG	MK	NPA	Hirshfeld	GAPT	Mulliken	Index
Hexane <sup>f</sup>	C <sub>(1)</sub>	−0.093	−0.061	−0.082	−0.39	−0.059	0.083	−0.212	138
	C <sub>(2)</sub>	−0.111	0.247	0.264	−0.393	−0.059	0.105	−0.304	139
	C <sub>(3)</sub>	−0.145	−0.249	−0.319	−0.592	−0.1	0.058	−0.864	140
	H <sub>(1)</sub>	0.034	0.005	0.012	0.193	0.03	−0.042	0.198	141
	H <sub>(2)</sub>	0.037	−0.049	−0.041	0.193	0.031	−0.043	0.168	142
	H <sub>(3)</sub>	0.073	0.051	0.069	0.205	0.033	−0.032	0.212	143
	H <sub>(4)</sub>	0.066	0.05	0.069	0.199	0.032	−0.021	0.218	144
CH <sub>3</sub> −CCl <sub>3</sub>	C(CCl <sub>3</sub> )	0.398	−0.115	−0.338	−0.119	0.169	1.044	0.671	145
	C(CH <sub>3</sub> )	−0.261	−0.327	−0.546	−0.654	−0.094	−0.113	−0.737	146
	H	0.093	0.155	0.236	0.237	0.052	0.035	0.305	147
	Cl	−0.139	−0.008	0.059	0.02	−0.077	−0.346	−0.283	148
1,4-Dioxane <sup>e</sup>	C	0.116	0.081	0.033	−0.082	0.009	0.42	−0.229	149
	H(eq)	0.065	0.049	0.068	0.192	0.047	−0.015	0.279	150
	H(ax)	0.046	0.053	0.071	0.164	0.031	−0.055	0.221	151
	O	−0.453	−0.366	−0.342	−0.548	−0.173	−0.7	−0.542	152
	C(C=O)	0.172	0.716	0.786	0.584	0.168	0.82	0.51	153
(CH <sub>3</sub> ) <sub>2</sub> CO	C(CH <sub>3</sub> )	−0.199	−0.411	−0.579	−0.714	−0.1	−0.129	−0.655	154
	H(CH <sub>3</sub> <sup>inpla</sup> )	0.085	0.116	0.159	0.235	0.048	0.021	0.226	155
	H(CH <sub>3</sub> <sup>opla</sup> )	0.094	0.105	0.149	0.228	0.05	0.019	0.246	156
	O	−0.322	−0.545	−0.544	−0.539	−0.263	−0.682	−0.636	157
	C(CHO)	0.156	0.585	0.591	0.442	0.147	0.776	−0.026	158
HCH <sub>3</sub> CO	C(CH <sub>3</sub> )	−0.188	−0.381	−0.51	−0.725	−0.098	−0.124	−0.552	159
	H(CHO)	0.087	−0.047	−0.038	0.093	0.039	−0.072	0.413	160
	H(CH <sub>3</sub> <sup>inpla</sup> )	0.087	0.088	0.124	0.216	0.045	0.008	0.245	161
	H(CH <sub>3</sub> <sup>opla</sup> )	0.094	0.124	0.16	0.244	0.057	0.035	0.231	162
	O	−0.33	−0.494	−0.487	−0.515	−0.248	−0.659	−0.543	163
Cyclopropane	C	−0.124	−0.2	−0.282	−0.418	−0.083	0.003	−0.555	164
	H	0.062	0.1	0.141	0.209	0.042	−0.001	0.278	165
Cyclohexane <sup>e</sup>	C	−0.088	0.035	−0.035	−0.395	−0.061	0.087	−0.347	166
	H(ax)	0.041	−0.013	0.011	0.191	0.032	−0.041	0.155	167
	H(eq)	0.047	−0.022	0.024	0.204	0.029	−0.045	0.192	168

<sup>a</sup> **CH<sub>3</sub>−CC−CN**: C<sub>(4)</sub>H<sub>3</sub>−C<sub>(2)</sub>−C<sub>(1)</sub>−C<sub>(3)</sub>N<sup>b</sup> **Butadiene**: backbone chain C<sub>(1)</sub>−C<sub>(2)</sub>−C<sub>(2)</sub>−C<sub>(1)</sub>; H<sub>(1)</sub> = H bonded to C<sub>(2)</sub>; H<sub>(2)</sub> = H bonded to C<sub>(1)</sub> in cis position with respect to C<sub>(2)</sub>; H<sub>(3)</sub> = H bonded to C<sub>(1)</sub> in trans position with respect to C<sub>(2)</sub><sup>c</sup> **H<sub>2</sub>C−CH−CH<sub>3</sub>**: C<sub>(1)</sub>=C(CH<sub>2</sub>); C<sub>(2)</sub>=C(CH); C<sub>(3)</sub>=C(CH<sub>3</sub>); H<sub>(1)</sub>=H(CH); H<sub>(2)</sub>=H bonded to C<sub>(1)</sub> in trans position with respect to H<sub>(1)</sub>; H<sub>(3)</sub>=H bonded to C<sub>(1)</sub> in trans position with respect to C<sub>(3)</sub>; H<sub>(4)</sub>=H(CH<sub>3</sub> inpla); H<sub>(5)</sub>=H(CH<sub>3</sub> oppla)<sup>d</sup> H(G) = H in gauche position with respect to the O lone pair; H(T) = H in trans position with respect to the O lone pair<sup>e</sup> H(eq) = H in CH bonds with equatorial direction with respect to the molecule, H(ax) = H in CH bonds with axial direction<sup>f</sup> **CH<sub>3</sub>−(CH<sub>2</sub>)<sub>3</sub>−CH<sub>3</sub>**: backbone chain C<sub>(1)</sub>−C<sub>(2)</sub>−C<sub>(3)</sub>−C<sub>(2)</sub>−C<sub>(1)</sub>; H<sub>(1)</sub>=H[C<sub>(1)</sub>H<sub>3</sub> inpla]; H<sub>(2)</sub>=H[C<sub>(1)</sub>H<sub>3</sub> oppla]; H<sub>(3)</sub>=H[C<sub>(2)</sub>H<sub>2</sub>]; H<sub>(4)</sub>=H[C<sub>(3)</sub>H<sub>2</sub>]; **CH<sub>3</sub>−(CH<sub>2</sub>)<sub>4</sub>−CH<sub>3</sub>**: backbone chain C<sub>(3)</sub>−C<sub>(2)</sub>−C<sub>(1)</sub>−C<sub>(1)</sub>−C<sub>(2)</sub>−C<sub>(3)</sub>; H<sub>(1)</sub>=H[C<sub>(1)</sub>H<sub>2</sub>]; H<sub>(2)</sub>=H[C<sub>(2)</sub>H<sub>2</sub>]; H<sub>(3)</sub>=H[C<sub>(3)</sub>H<sub>3</sub> inpla]; H<sub>(4)</sub>=H[C<sub>(3)</sub>H<sub>3</sub> oppla]<sup>g</sup> Not available in Gaussian

hand, for most of the molecules reported in Table 1, the charge distribution provided by GAPT charges is very different from that given by IR charges: Indeed, the presence of charge fluxes in GAPT charges is often unavoidable, while it is minimized in IR charges. Looking to RMS and MAD values for atoms different from hydrogen

(Table 3), we can realize that the GAPT method gives very different values of O, Cl and F charges; moreover, GAPT charges on C atoms are almost always larger than IR charges, while on the contrary H charges are smaller.

By analyzing the plots reported in Fig. 1, it can be seen that in the case of ESP methods, a good agreement with IR

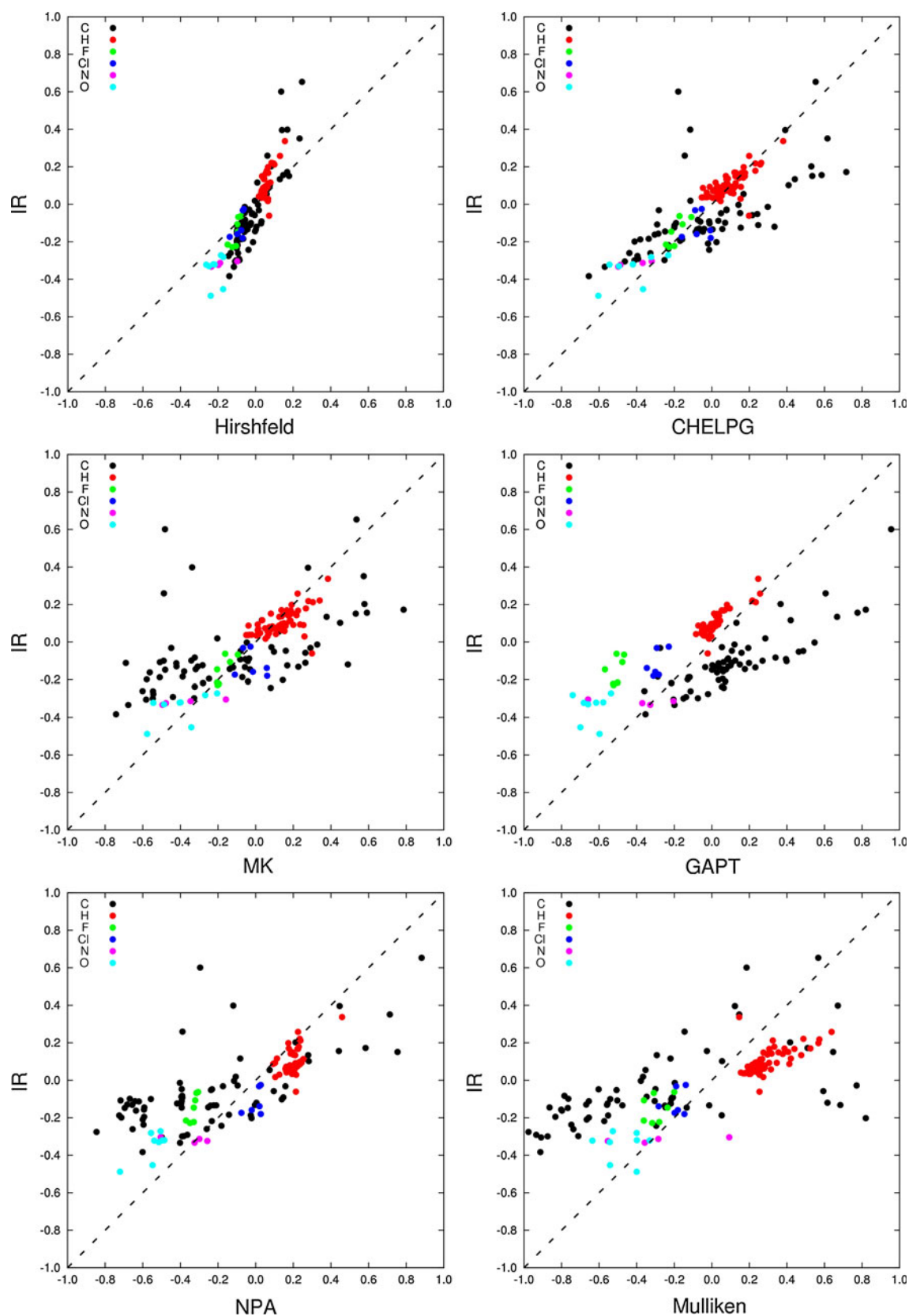


**Fig. 1** Correlation plots of IR charges with respect to those obtained with other methods discussed in this work. Units are electron charge. Different colors have been used to distinguish charges belonging to different kinds of atoms

**Table 2** RMS deviation and mean absolute deviation (MAD) of IR charges with respect to the other charges discussed in this paper

	RMS	MAD
Hirshfeld	0.107	0.079
CHELPG	0.157	0.104
MK	0.220	0.144
NPA	0.243	0.185
GAPT	0.257	0.190
Mulliken	0.377	0.292

charges is obtained in particular for charges on F, O and H, while the most relevant discrepancies are found for C atoms, in particular when the MK scheme is applied; the spread of charge values is more limited in the case of Hirshfeld charges. These results are confirmed also by the RMS and MAD values reported in Table 3 demonstrating that CHELPG, MK and Hirshfeld methods are the ones showing the least deviation with respect to IR charges in the case of F, H, C and O atoms. In particular, for F and O atoms, the ESP method gives charges more similar to the IR ones; on the other side, IR charges on C atoms are in very good agreement with Hirshfeld charges. This latter feature is particularly interesting since ESP methods are known to be less reliable in predicting the charge of the innermost atoms in molecules [19, 20]. For Cl and N atoms, a good agreement is obtained also when considering Mulliken and NPA charges but, since just a few molecules containing N and Cl atoms have been considered, we cannot draw a general conclusion.

So far, the performance of IR charges has been simply discussed by comparison with other charges; in the following, we would like to verify whether trends related to intramolecular effects are correctly reproduced.

IR charges effectively describe the changes in polarity of the CH bonds while varying the hybridization state of the C atom, indeed ethane ( $q_{\text{H}}^{\text{IR}} = 0.070$  e), ethylene ( $q_{\text{H}}^{\text{IR}} = 0.149$  e) and acetylene ( $q_{\text{H}}^{\text{IR}} = 0.218$  e) show increasing polarity. Moreover, the H charges belonging to sp systems are quite large ( $>0.2$  e), in agreement with their capability to form hydrogen bonding.

Also, more subtle effects such as hyperconjugation, observed for  $-\text{CH}_3$  groups attached to conjugated systems [58–60], are correctly displayed, as shown by the H charges of  $\text{CH}_3\text{--C}_2\text{--CH}_3$  ( $q_{\text{H}}^{\text{IR}} = 0.096$  e) and acetone ( $q_{\text{H}}^{\text{IR}} = 0.090$  e), both exhibiting larger values with respect to the H atoms of ethane. Another peculiar intramolecular effect, namely the backdonation of electronic charge from lone pairs of electronegative atoms (e.g., O) [58, 61, 62], is correctly described as it is found in formaldehyde ( $q_{\text{H}}^{\text{IR}} = 0.093$  e to be compared to  $q_{\text{H}}^{\text{IR}} = 0.149$  e in  $\text{C}_2\text{H}_4$ ), methanol and dimethylether which show, for the out of plane H atoms in trans position with respect to the oxygen lone pairs (0.062 and 0.055 e, respectively), lower charges than those of H atoms in gauche position (0.080 and 0.078 e). These features were demonstrated also on the basis of experimental IR intensities [25, 35, 58–62].

Regarding the other models, we can observe that the effect of carbon hybridization on the CH polarity is described correctly by every method except NPA, for

**Table 3** RMS deviation and mean absolute deviation (MAD) of IR charges with respect to those obtained with other methods. Charges for C, H, F, Cl, O and N atoms are considered separately

Carbon			Hydrogen			Fluorine		
	RMS	MAD		RMS	MAD		RMS	MAD
Hirshfeld	0.135	0.102	CHELPG	0.057	0.042	MK	0.048	0.040
CHELPG	0.230	0.179	Hirshfeld	0.069	0.055	CHELPG	0.056	0.046
MK	0.327	0.261	MK	0.077	0.055	Hirshfeld	0.068	0.055
NPA	0.344	0.284	GAPT	0.090	0.086	Mulliken	0.161	0.145
GAPT	0.351	0.281	NPA	0.119	0.106	NPA	0.189	0.181
Mulliken	0.542	0.462	Mulliken	0.203	0.192	GAPT	0.365	0.360
Chlorine			Oxygen			Nitrogen		
	RMS	MAD		RMS	MAD		RMS	MAD
Hirshfeld	0.063	0.057	MK	0.118	0.103	NPA	0.106	0.073
CHELPG	0.098	0.081	CHELPG	0.123	0.109	CHELPG	0.119	0.100
Mulliken	0.101	0.083	Hirshfeld	0.154	0.133	MK	0.134	0.123
NPA	0.130	0.117	Mulliken	0.175	0.146	Hirshfeld	0.144	0.138
MK	0.143	0.114	NPA	0.204	0.198	GAPT	0.187	0.129
GAPT	0.183	0.175	GAPT	0.305	0.290	Mulliken	0.230	0.170



which very close and high charge values of 0.191 and 0.200 e are calculated for  $C_2H_4$  and  $C_2H_6$ , respectively. For the same molecules, IR charges are numerically very similar to ESP charges (CHELPG and MK), while the variation of Hirshfeld charges describe the correct chemical trends but with a very limited spread (from 0.033 to 0.096 e). In particular, the low value obtained for the H charge in  $C_2H_2$  does not describe the acidic character of this H atom, which is able to form hydrogen bonds. In the case of hyperconjugation, the effect is found (and maybe overestimated) when ESP charges are considered (see for instance acetone). On the other side, Hirshfeld charges describe again the correct trend but show a quite small charge increase, similarly to IR charges. As for backdonation, we find that the effect is again emphasized by ESP charges, so that negative H charges are found for methanol and formaldehyde (CHELPG scheme). Also in the case of GAPT charges, all the values calculated for H affected by backdonation are negative, due to the very large (and negative) charge fluxes occurring in these cases.

Another trend is shown by charges on C atoms when bonded to halogen atoms [13, 21]: Considering the case of halomethanes and based simply on the electronegativity scale ( $H < Br < Cl < F$ ), we expect that in mono-substituted methanes, the charge of C atom should show an increasing negative value while decreasing the electronegativity of the substituent. Indeed, in  $CH_3F$   $q_C^{IR} = -0.003$  e, in  $CH_3Cl$   $q_C^{IR} = -0.100$  e, in  $CH_3Br$   $q_C^{IR} = -0.112$  e and finally in methane  $q_C^{IR} = -0.276$  e. Furthermore, a similar effect is expected and observed when increasing the number of halogen atoms: Indeed, in  $CH_2F_2$   $q_C^{IR} = 0.396$  e and in  $CHF_3$   $q_C^{IR} = 0.653$  e, while a similar behavior is also shown by chloromethanes. The trends for C charges commented above are reproduced also by the other methods here considered: In particular, both ESP and GAPT predict a very large spread of values for the C atom (for instance, for CHELPG  $q_C = -0.396$  e in  $CH_4$  and  $q_C = +0.142$  e for  $CH_3F$ , for GAPT  $q_C = -0.020$  e for  $CH_4$  and  $q_C = 0.547$  e for  $CH_3F$ ). Hirshfeld charges display a more limited variation (from  $-0.144$  to  $0.013$  e), while IR charges present numerical values lying between ESP and Hirshfeld charges (from  $-0.276$  to  $-0.003$  e). When considering the C atom charges of fluoromethanes, IR charges show large variation while increasing the number of fluorine atoms, from  $CH_3F$  ( $-0.003$  e) to  $CHF_3$  ( $0.653$  e), similarly to ESP methods, while the variation observed for Hirshfeld charges is again more limited (from  $0.013$  to  $0.247$  e). Both NPA and GAPT charges are very large and seemingly unrealistic: In particular, GAPT charges of C atoms are almost additive with the number of F atoms (from  $0.547$  to  $1.591$  e).

For chlorine substituted methanes, different results are found: ESP charges on C atoms do not predict the expected trend in these cases, while Hirshfeld and IR charges do; Hirshfeld charges, however, show a quite limited variation (from  $-0.025$  e for  $CH_3Cl$  to  $0.136$  e for  $CHCl_3$ ), and a larger variation is found for IR charges (from  $-0.100$  to  $0.601$  e). GAPT charges still show very large and seemingly unrealistic values (from  $0.270$  to  $0.955$  e).

#### 4.3 Application to some critical cases

As already discussed in Sect. 3.2, for non-planar molecules, there are several cases where both the choice of a local plane and the set of atoms to be corrected cannot be made unambiguously. Luckily, in most cases, different choices provide quite similar pictures: This happens for instance in the case of ethylene oxide where the definition of the hydrogen charge can be made selecting the H–C–O plane (data reported in Table 1) or the H–C–C plane.<sup>4</sup> The second choice determines the following set of charges:  $q_C^{IR} = -0.002$  e;  $q_H^{IR} = 0.067$  e;  $q_O^{IR} = -0.265$  e, which has to be compared with the set  $q_C^{IR} = 0.019$  e;  $q_H^{IR} = 0.058$  e;  $q_O^{IR} = -0.272$  e, from Table 1.

An even better agreement is found in the case of butane where there are two choices for the definition of the local plane relative to the hydrogen atoms of the methylene group. Comparing the charges reported in Table 1 (local plane containing the carbon atom of the methyl group, values in parentheses) to the charges obtained choosing the local plane that contains the two methylene carbon atoms, we obtain the following results:  $q_C^{IR}(\text{CH}_3) = -0.153$  e ( $-0.157$  e);  $q_C^{IR}(\text{CH}_2) = -0.121$  e ( $-0.125$  e);  $q_H^{IR}(\text{CH}_3, \text{inpla}) = 0.073$  e ( $0.073$  e);  $q_H^{IR}(\text{CH}_3, \text{opla}) = 0.066$  e ( $0.066$  e);  $q_H^{IR}(\text{CH}_2) = 0.034$  e ( $0.038$ ). As for the correction procedure, in the case of butane, only one correction parameter can be introduced, because of the vanishing dipole moment: It seemed reasonable in this case to correct all carbon charges, which can form one subset, even if they are not strictly equivalent.

Other cases for which different choices of the local planes give different but qualitatively similar pictures are 1,4 dioxane and  $CH_3CCl_3$  for which the data reported in Table 1 have been obtained by selecting the three  $\beta$ -A–B atoms on the basis of their electronegativity, for example H–C–O for the H charge in dioxane and Cl–C–Cl for the chlorine charge of  $CH_3CCl_3$ .

However, in a few peculiar cases, critical situations appear, even if the procedure for the local plane selection and charge correction is carefully undertaken and different

<sup>4</sup> In both cases, following the guidelines illustrated in Sect. 3.2, the corrections have been applied to oxygen and to carbon charges.

choices (if available) are analyzed. Generally speaking, some problems are expected to arise when tetrahedral carbon atoms carry more than one electron rich substituents, as in the case of halogenated methanes. In these cases, it may happen that bending charge fluxes on halogen atoms are so relevant (compared with the small values of hydrogen charges) that it is practically impossible to obtain  $q_H^{IR}$  values reasonably free from flux contributions. On the other hand, for these cases, the two available conditions for charge correction should be used in order to adjust the carbon charge (inner atom) and that of the electron rich halogen atoms.

For the above reasons, it is difficult to state whether the decrease in the IR hydrogen charge in the series  $\text{CH}_3\text{F}$  ( $q_H^{IR} = 0.072$  e),  $\text{CH}_2\text{F}_2$  ( $q_H^{IR} = 0.030$  e),  $\text{CHCF}_3$  ( $q_H^{IR} = 0.017$  e) has to be regarded as the consequence of an increasingly relevant charge backdonation as far as the number of backdonating fluorine atoms increases. It is indeed possible that the trend obtained is simply due to the error determined by the unavoidable presence of charge flux contributions, which became more and more important, thanks to the existence of one (or two) fluorine atoms lying out of the local plane containing the CH bond. Perhaps, this second explanation can also justify the fact that hydrogen infrared charges (see Table 1) decrease in their values passing from  $\text{CH}_3\text{Cl}$  ( $q_H^{IR} = 0.091$  e) to  $\text{CH}_2\text{Cl}_2$  ( $q_H^{IR} = 0.029$  e) down to a negative value in the case of  $\text{CHCl}_3$  ( $q_H^{IR} = -0.061$  e). This behavior does not agree with the expectation of an increasingly large inductive effect<sup>5</sup> (while increasing the number of the electronegative substituents), which on the contrary is captured by CHELPG and MK charges and to a lesser extent by Hirshfeld charges.

## 5 Summary and conclusions

The idea of extracting atomic charges from IR intensity parameters comes back to some decades ago and has found a wide interest among vibrational spectroscopists. Apart from the GAPT schemes and some early methods [36, 37] adopted to connect ECCF to quantum chemical calculations, no generalizations have been proposed to extract charges from APT following a procedure suitable for computer implementation and for usage also by non-experts. In this paper, we have presented an attempt for such an implementation by considering in detail the method and comparing the results obtained with other popular schemes for the calculation of atomic charges.

<sup>5</sup> The backdonation effect from chlorine lone pairs is expected to be less effective with respect to that from fluorine lone pairs because of energetic reasons.

The IR charge method so derived has a number of advantages:

1. IR charges rely on a solid background since they can be related to experimental quantities (IR intensities).
2. For planar molecules, they give a theoretically sound and unambiguous description of the molecular charge distribution [46].
3. The comparison with other methods and the good agreement obtained with Hirshfeld and ESP charges demonstrate that IR charges are an appealing alternative to the commonly used schemes. Furthermore, they provide a description of molecular charge distribution which follows the “chemical intuition” as demonstrated by testing on a set of about fifty molecules. Referring in particular to Hirshfeld charges, whose reliability has been investigated and demonstrated in different papers [13, 21], IR charges gave a similar and sound description of chemical trends while giving a larger numerical spread, in better agreement with expectations.
4. The comparison with other charges obtained from APTs (e.g., GAPT charges) demonstrates that IR charges have sounder definition and physical meaning.
5. As a final point, a further analysis of APT components would allow to extract information on charge fluxes [43, 44], thus offering a more detailed description of both static and dynamic molecular charge distribution: Also in this case, general methods are lacking, while they are desirable for a painless calculation of these parameters.

Despite these general advantages, the present method still presents some drawbacks and possible disadvantages:

1. For non-planar systems, the model can be generalized to obtain an approximate definition of atomic charge. However, the application of the method is not always univocally defined.
2. In some cases, it is impossible to find a local plane suitable to obtain a good description of the molecular charge distribution. According to our tests, this deficiency affects only a very limited number of cases.
3. The calculation of IR charges (or GAPT charges) requires the knowledge of APT components, and hence an IR intensity calculation has to be carried out. The computational cost of such a calculation is much higher than the simple geometry optimization required by other schemes (ESP, Hirshfeld...) and thus, in principle, smaller molecular systems can be investigated by using similar computational resources and/or times. In any case, this limitation is negligible when IR spectra need to be computed anyway: In these cases, the determination of IR charges offers a further advantage since they allow a rationalization of the effects observed on IR intensities. Concerning the

application on large molecular systems, IR charges can be calculated on all molecules whose dimensions allow the calculation of IR spectra.

This work opens the way to many possible follow-ups: On the one hand, it will be interesting to extend the analysis of IR charge values to a wider variety of molecular systems, and on the other hand, the prediction of reliable IR charges depends on the choice of a suitable quantum chemical method (or DFT functional) for the prediction of accurate IR intensities, which obviously requires testing.

## References

- Cho K, Kang YK, No KT, Scheraga HA (2001) *J Phys Chem B* 105:3624–3634
- Thomas A, Milon A, Brasseur R (2004) *Proteins* 56:102–109
- Duan Y, Wu C, Chowdhury S, Lee MC, Xiong G, Zhang W, Yang R, Cieplak P, Luo R, Lee T, Caldwell J, Wang J, Kollman P (2003) *J Comput Chem* 24:1999–2012
- Kang YK, Scheraga H (2008) *J Phys Chem B* 112:5470–5478
- Allen MP, Tildesley TJ (1987) *Computer simulation of liquids*. Clarendon Press, Oxford
- Mulliken RS (1955) *J Chem Phys* 23:1833–1840
- Lowdin PO (1950) *J Chem Phys* 18:365–375
- Lowdin PO (1970) *Adv Quantum Chem* 5:185–199
- Reed AE, Curtiss LA, Weinhold F (1988) *Chem Rev* 88:899–926
- Reed AE, Weinstock RB, Weinhold F (1985) *J Chem Phys* 83:735–746
- Bader RFW (1991) *Chem Rev* 91:893–928
- Hirshfeld FL (1977) *Theor Chem Acc* 44:129–138
- Guerra CF, Handgraaf JW, Baerends EJ, Bickelhaupt FM (2004) *J Comput Chem* 25:189–210
- Besler BH, Merz KM Jr, Kollman PA (1990) *J Comp Chem* 11:431–439
- Singh UC, Kollman PA (1984) *J Comp Chem* 5:129–145
- Chirlian LE, Franci MM (1990) *J Comp Chem* 8:894–905
- Breneman CM, Wiberg KB (1990) *J Comp Chem* 11:361–373
- De Proft F, Martin JML, Geerling P (1996) *Chem Phys Lett* 250:393–401
- Martin F, Zipse H (2005) *J Comput Chem* 26:97–105
- Hu H, Yang W (2007) *J Chem Theor Comput* 3:1004–1013
- De Proft F, Van Alsenoy C, Peeters A, Langenaeker W, Geerlings P (2002) *J Comput Chem* 23:1198–1209
- Sigfridsson E, Ryde U (1998) *J Comput Chem* 19:377–395
- De Proft F, Geerlings P, Martin JML (1996) In: Seminario JM (ed) *Recent developments and applications of modern density functional theory*. Elsevier Science BV, Amsterdam
- Person WB, Zerbi G (1982) *Vibrational intensities in infrared and Raman spectroscopy*. Elsevier Scientific publishing company, Amsterdam
- Gussoni M, Castiglioni C, Zerbi G (2001) In: Chalmers J, Griffiths P (eds) *Handbook of vibrational spectroscopy*. Wiley, Chichester, UK and references therein
- Gribov LA (1964) *Intensity theory for infrared spectra of polyatomic molecules*. Consultant's Bureau, New York
- Gussoni M, Abbate S (1976) *J Chem Phys* 65:3489–3495
- Gussoni M (1985) *Prik Spectroscop* XLII: 265
- Decius JC (1975) *J Mol Spectrosc* 57:348–362
- Van Straten AJ, Smit WM (1976) *J Mol Spectrosc* 62:297–312
- King WT, Mast GB (1976) *J Phys Chem* 80:2521–2525
- Gussoni M, Castiglioni C, Zerbi G (1984) *J Phys Chem* 88:600–604
- Biarge JF, Herranz J, Morcillo J (1961) *Ann Fis Quim* A57:81
- Person WB, Newton JB (1964) *J Chem Phys* 61:1040–1049
- Gussoni M, Castiglioni C, Ramos MN, Rui M, Zerbi G (1990) *J Mol Struct* 224:445–470
- Gussoni M, Ramos MN, Castiglioni C, Zerbi G (1987) *Chem Phys Lett* 142:515–518
- Ramos MN, Gussoni M, Castiglioni C, Zerbi G (1988) *Chem Phys Lett* 151:397–402
- Haiduke RLA, Bruns RE (2005) *J Phys Chem A* 109:2680–2688
- Da Silva JV, Haiduke RLA, Bruns RE (2006) *J Phys Chem A* 110:4839–4845
- Da Silva JV, Faria SHDM, Haiduke RLA, Bruns RE (2007) *J Phys Chem A* 111:515–520
- Faria SHDM, Da Silva JV, Haiduke RLA, Vidal LN, Vazquez PAM, Bruns RE (2007) *J Phys Chem A* 111:7870–7875
- Cioslowski J (1989) *J Am Chem Soc* 111:8333–8336
- Milani A, Castiglioni C (2010) *J Phys Chem A* 114:624–632
- Milani A, Galimberti G, Castiglioni C, Zerbi G (2010) *J Mol Struct* 976:342–349
- Milani A, Castiglioni C (2010) *J Mol Struct Theorchem* 955:158–164
- Dinur U, Hagler AT (1989) *J Chem Phys* 91:2949–2970
- Gussoni M, Castiglioni C, Zerbi G (1984) *J Chem Phys* 80:1377–1381
- Gussoni M, Castiglioni C, Zerbi G (1983) *Chem Phys Lett* 99:101–106
- Castiglioni C, Gussoni M, Zerbi G (1984) *J Chem Phys* 80:3916–3918
- Araujo RCMU, Da Silva JBP, Ramos MN (1995) *Spectrochim Acta A* 51:821–830
- Rusu VH, Da Silva JBP, Ramos MN (2008) *Vib Spectrosc* 46:52–56
- Lopes KC, Pereira FS, De Araujo RCMU, Ramos MN (2001) *J Mol Struct* 417:565–566
- Ramos MN, Lopes KC, Silva WL, Tavares AM, Castriani FA, Do Monte SA, Ventura E, Araujo RCMU (2006) *Spectrochim Acta A* 63:383–390
- Wilson EB, Decius JC, Cross PC (1955) *Molecular vibrations*. McGraw Hill, New York
- Adamo C, Barone V (1999) *J Chem Phys* 110:6158–6169
- Gaussian 03, Revision C.01, Frisch MJ, Trucks GW, Schlegel HB, Scuseria GE, Robb MA, Cheeseman JR, Montgomery Jr. JA, Vreven T, Kudin KN, Burant JC, Millam JM, Iyengar SS, Tomasi J, Barone V, Mennucci B, Cossi M, Scalmani G, Rega N, Petersson GA, Nakatsuji H, Hada M, Ehara M, Toyota K, Fukuda R, Hasegawa J, Ishida M, Nakajima T, Honda Y, Kitao O, Nakai H, Klene M, Li X, Knox JE, Hratchian HP, Cross JB, Bakken V, Adamo C, Jaramillo J, Gomperts R, Stratmann RE, Yazyev O, Austin AJ, Cammi R, Pomelli C, Ochterski JW, Ayala PY, Morokuma K, Voth GA, Salvador P, Dannenberg JJ, Zakrzewski VG, Dapprich S, Daniels AD, Strain MC, Farkas O, Malick DK, Rabuck AD, Raghavachari K, Foresman JB, Ortiz JV, Cui Q, Baboul AG, Clifford S, Cioslowski J, Stefanov BB, Liu G, Liashenko A, Piskorz P, Komaromi I, Martin RL, Fox DJ, Keith TM, Al-Laham MA, Peng CY, Nanayakkara A, Challacombe M, Gill PMW, Johnson B, Chen W, Wong MW, Gonzalez C, Pople JA (2004) *Gaussian, Inc., Wallingford, CT*
- Gaussian 09, Revision A.1, Frisch MJ, Trucks GW, Schlegel HB, Scuseria GE, Robb MA, Cheeseman JR, Scalmani G, Barone V, Mennucci B, Petersson GA, Nakatsuji H, Caricato M, Li X, Hratchian HP, Izmaylov AF, Bloino J, Zheng G, Sonnenberg JL, Hada M, Ehara M, Toyota K, Fukuda R, Hasegawa J, Ishida M, Nakajima T, Honda Y, Kitao O, Nakai H, Vreven T, Montgomery Jr. JA, Peralta JE, Ogliaro F, Bearpark M, Heyd JJ, Brothers E,

- Kudin KN, Staroverov VN, Kobayashi R, Normand J, Raghavachari K, Rendell A, Burant JC, Iyengar SS, Tomasi J, Cossi M, Rega N, Millam NJ, Klene M, Knox JE, Cross JB, Bakken V, Adamo C, Jaramillo J, Gomperts R, Stratmann RE, Yazyev O, Austin AJ, Cammi R, Pomelli C, Ochterski JW, Martin RL, Morokuma K, Zakrzewski VG, Voth GA, Salvador P, Dannenberg JJ, Dapprich S, Daniels AD, Farkas Ö, Foresman JB, Ortiz JV, Cioslowski J, Fox DJ (2009) Gaussian, Inc., Wallingford, CT
58. Castiglioni C, Gussoni M, Zerbi G (1989) *J Mol Struct* 198:475–488
59. Castiglioni C, Gussoni M, Zerbi G (1986) *J Mol Struct* 141:341–346
60. Jona P, Gussoni M, Zerbi G (1981) *J Phys Chem* 85:2210–2218
61. Da Costa NB, Aquino AJA, Ramos MN, Castiglioni C, Zerbi G (1994) *J Mol Struct (Theochem)* 305:19–25
62. Castiglioni C, Gussoni M, Zerbi G (1985) *J Chem Phys* 82:3534–3541